

Surface Properties of Classical One-Component Plasma

Hiroo TOTSUJI*

(Received September 17, 1986)

SYNOPSIS

Surface properties of classical one-component plasma are investigated by numerical experiments on the system with periodicity in two directions perpendicular to the planar surface. The density profile, the electrostatic potential, the electric field, and the surface energy are obtained for intermediate values of the coupling parameter of bulk part Γ and compared with earlier experiments on spherical system. For $\Gamma = 10$, the surface energy is almost the same as earlier result. For $\Gamma = 1$, however, the surface energy is reduced about a factor of 2. The consistency of experimental values of the potential with the exact relation is checked and necessity of large system size is pointed out.

1. INTRODUCTION

The surface properties of the one-component plasma (OCP) have been studied as a model of the surface of the liquid metals or the interface of the electrode and the electrolyte solutions. Results of theoretical investigations based on integral equations or the density-functional method have been compared with those of numerical experiments.

In these investigations, some exact relationships between physical quantities have been found and are used to confirm the validity of theoretical results. The results of numerical experiments

*Department of Electronics

have also provided useful informations.

In numerical experiments by Badiali et al.⁽¹⁾ and by Levesque et al.⁽²⁾, spherically symmetric systems with a few hundred particles have been used to simulate the planar surface of OCP; the background charge is uniformly distributed in a sphere and a hard wall is placed to prevent the particles from evaporating to infinity. The results seem to indicate that we can use systems with a few hundred ions to obtain surface properties.

Rosinberg et al.⁽³⁾ have made theoretical analyses and found discrepancies between the results of density-functional method and numerical experiment for small values of the coupling parameter and it is argued by Hasegawa et al.⁽⁴⁾ that the discrepancies are not due to approximate nature of the density-functional method but due to the finiteness of the system used in numerical experiments.

The purpose of this paper is to present the results of numerical experiments for plane geometry and compare them with those for spherical geometry.

2. INTERACTION ENERGY

In order to investigate the properties of the planar surface of the one-component plasma, we consider a system of charged particles of charge e and the background of opposite charges where the latter has a constant charge density $-en_b$ but occupies only the domain $|z| < L_z/2$. Thus the background has two surfaces $|z|=L_z/2$ which are perpendicular to the z -axis. We place no hard walls which prevent particles from escaping to $|z|=\infty$. In directions parallel to the surface, our system is translationally invariant.

To simulate infinite extensions in x - and y -directions, we impose the periodic boundary conditions along these directions and denote the period by L . Our unit cell therefore is the domain bounded by four planes $|x|=L/2$ and $|y|=L/2$ and includes N ions. The condition of overall charge neutrality $N=en_bL^2L_z$ is satisfied in our unit cell.

The interaction energy per unit cell U is given by

$$U = (1/2) \sum_{i \neq j} [v^s(\vec{r}_{ij}) + v^l(\vec{r}_{ij}) + v_1^z(z_{ij})] + N \sum_i v_2^z(z_i) - (\pi/3)N^2(e^2L_z/L^2) + (N/2)U_M, \quad (1)$$

where $\vec{r}_{ij} = \vec{r}_i - \vec{r}_j$, $z_{ij} = z_i - z_j$,

$$v^s(\vec{r}) = e^2 \sum_{\vec{p}} \operatorname{erfc}[G\sqrt{(\vec{R}-\vec{p})^2+z^2}]/\sqrt{(\vec{R}-\vec{p})^2+z^2}, \quad (2)$$

$$v^l(\vec{r}) = \pi(e^2/L) \sum_{\vec{k} \neq 0} \exp(i\vec{k} \cdot \vec{R}) [\exp(K|z|) \operatorname{erfc}(K/2G+G|z|) + \exp(-K|z|) \operatorname{erfc}(K/2G-G|z|)]/KL, \quad (3)$$

$$v_1^z(z) = 2\pi(e^2/L) [-\exp(-G^2z^2)/\pi^{1/2}GL + (|z|/L) \operatorname{erfc}(G|z|) - |z|/L], \quad (4)$$

$$v_2^z(z) = 2\pi(e^2L_z/L^2) [(z^2/L_z^2 + 1/4) \theta(L_z/2 - |z|) + (|z|/L_z) \theta(|z| - L_z/2)], \quad (5)$$

and

$$\operatorname{erfc}(x) = 2\pi^{-1/2} \int_x^\infty dt \exp(-t^2). \quad (6)$$

In these expressions, \vec{R} denotes the x- and y-components of \vec{r} and \vec{p} and \vec{k} are the lattice and reciprocal lattice vectors corresponding to the two-dimensional periodicity of our system in x- and y-directions, and $\theta(x)$ is the unit step function. The constant U_M is the Madelung energy of the square lattice of charges interacting via the Coulomb potential e^2/r in the uniform neutralizing background⁽⁵⁾;

$$U_M = -2 \cdot 1.950132 \dots (e^2/L). \quad (7)$$

To obtain (1) let us first assume our system to be periodic also in the z-direction with period L'_z and finally take the limit $L'_z \rightarrow \infty$. The electrostatic potential $\phi(\vec{R}, z)$ is given by

$$\phi(\vec{R}, z) = (L^2 L'_z)^{-1} \sum_{\vec{k}} [4\pi/(K^2 + k_z^2)] \rho(\vec{k}) \exp(i\vec{k} \cdot \vec{r}), \quad (8)$$

where $\rho(\vec{k})$ is the Fourier component of the charge density $\rho(\vec{R}, z)$ ($\rho(\vec{k}=0)=0$) for $\vec{k}=(\vec{K}, k_z)$, the reciprocal lattice vector with $k_z=(2\pi/L'_z)n_z$, $n_z=0, \pm 1, \pm 2, \dots$. To obtain the interaction energy per unit cell, we subtract the self-interaction energy from the integral over the unit cell

$$U' = (1/2) \int_{L^2 L'_z} d\vec{r} \rho(\vec{r}) \phi(\vec{r}) = (2L^2 L'_z)^{-1} \sum_{\vec{k}} [4\pi/(K^2 + k_z^2)] |\rho(\vec{k})|^2$$

$$\begin{aligned}
& = (2L^2)^{-1} \sum_{ij} \sum_{\vec{K} \neq 0} (2\pi e^2/K) \exp(-i\vec{K} \cdot \vec{R}_{ij} - K|z_{ij}|) \\
& \quad + (2L^2 L'_z)^{-1} \sum_{k_z} (4\pi/k_z^2) |\rho(\vec{K}=0, k_z)|^2. \quad (9)
\end{aligned}$$

Here the summation with respect to k_z is performed for those terms with $\vec{K} \neq 0$ in the limit $L'_z \rightarrow \infty$. Separating the Madelung energy (7), the interaction energy per unit cell U is thus given as

$$\begin{aligned}
U & = (2L^2)^{-1} \sum_{i \neq j} \sum_{\vec{K} \neq 0} (2\pi e^2/K) \exp(-i\vec{K} \cdot \vec{R}_{ij} - K|z_{ij}|) \\
& \quad + (2L^2 L'_z)^{-1} \sum_{k_z} (4\pi/k_z^2) |\rho(\vec{K}=0, k_z)|^2 + (N/2)U_M. \quad (10)
\end{aligned}$$

The first term on the right hand side given as a series in the Fourier space can be transformed into a sum of rapidly converging series in both the real and the Fourier spaces. For this purpose we note the identities

$$\exp(-K|z|)/K = \pi^{-1/2} \int_0^\infty dt \exp(-K^2 t^2/4 - z^2/t^2), \quad (11)$$

$$L^{-2} \sum_{\vec{K}} 2\pi^{1/2} \exp(i\vec{K} \cdot \vec{R} - K^2 t^2/4 - z^2/t^2) = \sum_{\vec{P}} 2\pi^{-1/2} \exp\{-[z^2 + (\vec{R} - \vec{P})^2]/t^2\}/t^2 \quad (12)$$

and obtain, by dividing the integral into $(0, G^{-1})$ and (G^{-1}, ∞) ,

$$\begin{aligned}
& L^{-2} \sum_{\vec{K} \neq 0} (2\pi e^2/K) \exp(i\vec{K} \cdot \vec{R} - K|z|) \\
& = \pi (e^2/L) \sum_{\vec{K} \neq 0} [\exp(K|z|) \operatorname{erfc}(K/2G + G|z|) + \exp(-K|z|) \operatorname{erfc}(K/2G - G|z|)]/KL \\
& \quad + e^2 \sum_{\vec{P}} \operatorname{erfc}[G\sqrt{(\vec{R} - \vec{P})^2 + z^2}]/\sqrt{(\vec{R} - \vec{P})^2 + z^2} \\
& \quad - 2\pi^{1/2} (e^2/L) \exp(-G^2 L^2)/GL + 2\pi (e^2/L) (|z|/L) \operatorname{erfc}(G|z|). \quad (13)
\end{aligned}$$

Denoting the one-dimensional charge distribution $\int \int d\vec{R} \rho(\vec{R}, z)$ by $\rho(z)$ and taking the limit $L'_z \rightarrow \infty$, we rewrite the second term on the right hand side of (10) as

$$\begin{aligned}
& -(\pi/L^2) \int \int dz dz' \rho(z) \rho(z') |z - z'| = \pi (e^2 L_z/L^2) \left\{ - \sum_{ij} |z_{ij}|/L_z \right. \\
& \quad \left. + 2N \sum_i [(z_i^2/L_z^2 + 1/4) \theta(L_z/2 - |z|) + (|z_i|/L_z) \theta(|z| - L_z/2)] - N^2/3 \right\}. \quad (14)
\end{aligned}$$

From Eqs.(10), (13), and (14), we have finally (1).

3. RESULTS

We define the bulk coupling parameter Γ by

$$\Gamma = e^2 / ak_B T \quad (15)$$

where T is the temperature, k_B the Boltzmann constant, and $a = (3/4\pi n_b)^{1/3}$. The numerical experiments are performed for $\Gamma = 1, 2, 5,$ and 10 by the standard Monte Carlo method due to Metropolis et al.⁽⁶⁾ We assume $L_z = L$; the background occupies a cubic domain in our unit cell. The number of independent particles and the number of steps are summarized in Table 1. Our system has smaller value for the ratio of the surface area to the volume than spherical case. We therefore use 216 particles for the cases of $\Gamma = 2, 5,$ and 10 where the surface transition layer is relatively thin, and 512 particles for $\Gamma = 1$ where the layer has the thickness of more than $(5-6)a$. The initial steps of about half of those listed are discarded.

The density profiles are shown in Fig.1 and listed in Table 2. In figures and tables, the zero of the z -axis is taken at the surfaces of the background and the positive z -axis is in the direction outward from the surface. The center of the background is at $z = -4.836a$ for $N = 216$ and at $z = -6.448a$ for $N = 512$.

For $\Gamma = 2$, we observe the oscillation of the density profile. The amplitude of oscillation increases with the increase of Γ and, at the same time, the thickness of the transition layer outside the surface of the background becomes small.

Compared with the result for spherical geometry with $\Gamma = 1$ (Badiali et al.⁽¹⁾, Levesque et al.⁽²⁾, the density has larger value for the same value of z . This result is consistent with the prediction of the density-functional analyses^{(3),(4)}. For $\Gamma = 10$, the amplitude of the oscillation of the density profile is smaller than the spherical case. This tendency also seems to agree with density-functional analyses but the reliability of the square gradient expansion employed in the latter needs another confirmation.

The surface energy is obtained by subtracting the internal energy of the bulk OCP occupying the volume of the background from the experimental values of total internal energy. The results for the

Table 1. Experimental parameters

Γ	N	Number of steps
1	512	$3 \cdot 10^5$
2	216	$3 \cdot 10^5$
5	216	$3 \cdot 10^5$
10	216	$3 \cdot 10^5$

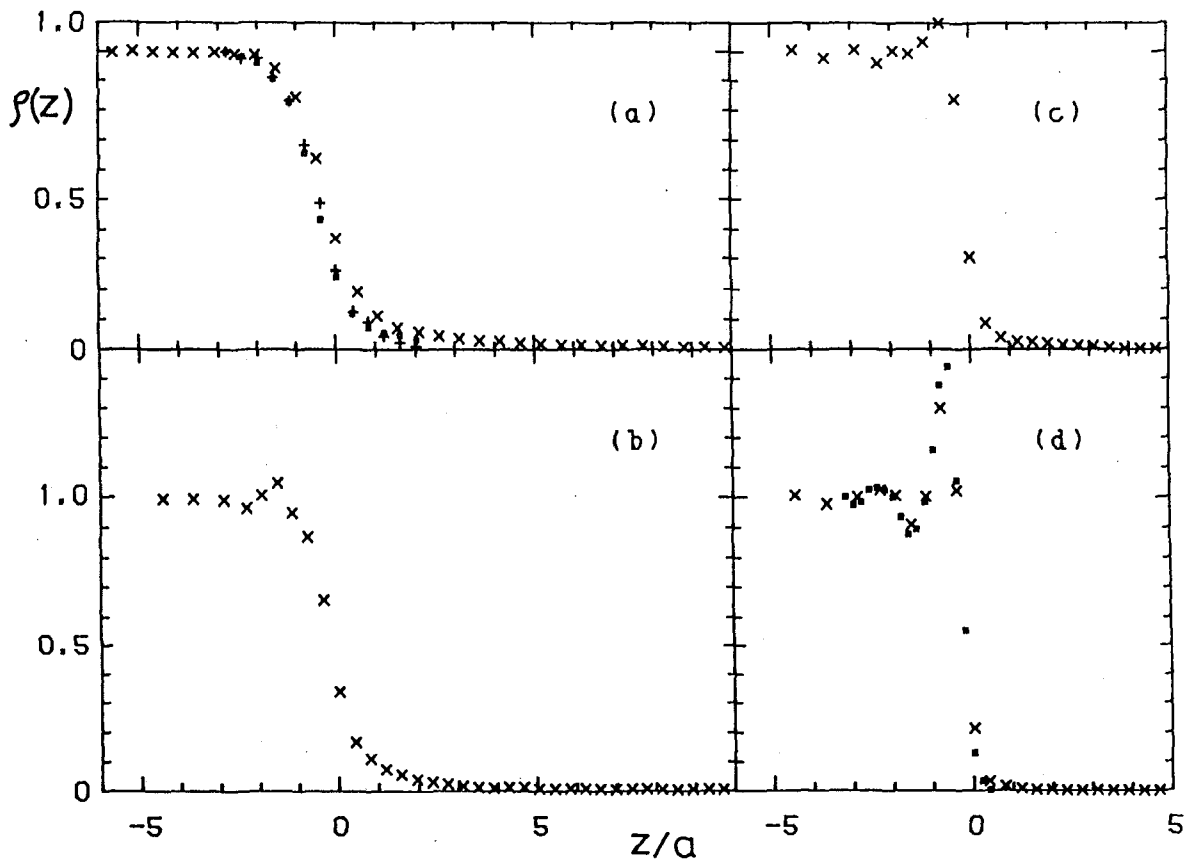


Fig.1. Density profile $\rho(z)$ for $\Gamma=1$ (a), 2(b), 5(c), and 10(d). Present results (x), those by Badiali et al.⁽¹⁾ (\square), and those by Levesque et al.⁽²⁾ (+) are plotted.

Table 2. Density profile

z/a	$\rho(z)$ $\Gamma = 1$	z/a	$\rho(z)$ $\Gamma = 2$	$\rho(z)$ $\Gamma = 5$	$\rho(z)$ $\Gamma = 10$
-6.19	1.005	-4.45	0.994	1.005	1.005
-5.67	0.998	-3.68	0.992	0.979	0.980
-5.16	1.001	-2.90	0.992	1.008	1.001
-4.64	1.000	-2.32	0.966	0.962	1.022
-4.13	0.995	-1.93	1.006	1.004	1.006
-3.61	0.996	-1.55	1.048	0.995	0.910
-3.10	0.999	-1.16	0.950	1.034	1.002
-2.58	0.993	-0.77	0.868	1.099	1.301
-2.06	0.988	-0.39	0.660	0.836	1.022
-1.55	0.942	0.00	0.340	0.305	0.214
-1.03	0.843	0.39	0.167	0.085	0.029
-0.52	0.638	0.77	0.110	0.039	0.013
0.00	0.370	1.16	0.073	0.025	0.006
0.52	0.190	1.55	0.055	0.024	0.002
1.03	0.110	1.93	0.038	0.020	0.001
1.55	0.071	2.32	0.029	0.015	
2.06	0.057	2.71	0.024	0.012	
2.58	0.045	3.10	0.017	0.009	
3.10	0.036	3.48	0.011	0.007	
3.61	0.029	3.87	0.009	0.003	
4.13	0.026	4.26	0.011	0.002	
4.64	0.021	4.64	0.013	0.002	
5.16	0.018				
5.67	0.016				
6.19	0.016				
6.71	0.014				
7.22	0.015				
7.74	0.011				
8.25	0.011				

surface energy are shown in Fig.2 and Table 3. Compared with the results of earlier experiments⁽¹⁾, the surface energy for $\Gamma=1$ is much reduced but the value for $\Gamma=10$ is in good agreement.

The electrostatic potential V and electric field E (which has only the z -component) are plotted in Fig.3 and Fig.4: We take the bulk potential to be zero. The result for the potential is summarized in Table 4.

There is an exact relation^{(7),(8)} between the potential and the bulk pressure P of OCP: In our case, we have

$$eV(0)/k_B T = P/n_b k_B T \quad . \quad (16)$$

Known values of the right hand side of the above relation⁽⁹⁾ are also listed in Table 4 and are shown also in Fig.3.

In the case of $\Gamma=1$ with $N=512$, the relation (16) is satisfied with sufficient accuracy. In other cases, however, the agreement is not satisfactory: The experimental values of the potential difference is always larger than expected from the exact relation. At the same time, the potential has positive second derivative and is not sufficiently flat in the central domain, except for the case of $N=512$. This means that the average charge density is slightly negative in the central part.

In Fig.1, the density profile seems to have achieved the asymptotic behavior in the central region. This fact, however, does not guarantee that the potential, which is the first moment of the charge density, also satisfies the asymptotic property. As a result, the electrostatic potential near the surface deviates from the correct value predicted by the exact relation.

The effect of this deviation on the surface energy may be estimated as follows. For a particle in the surface region, the microscopic potential energy is composed of the average part corresponding to the average density profile and the fluctuating part due to correlations. The surface energy is the difference of this potential energy and the bulk correlation energy per particle, summed over particles in the column perpendicular to the surface with the base of unit area and multiplied by $1/2$ to adjust double counting. Relative importance of the error in the average potential, ΔV , may then be estimated by evaluating the correlational part of the energy by the bulk OCP value with the density at the surface as

Table 3. Surface energy

Γ	$U_s/an_b k_B T$	
	present result	Badiali et al.
1	0.69 ± 0.04	1.309
2	0.78 ± 0.07	
5	0.71 ± 0.04	
10	0.47 ± 0.03	0.481

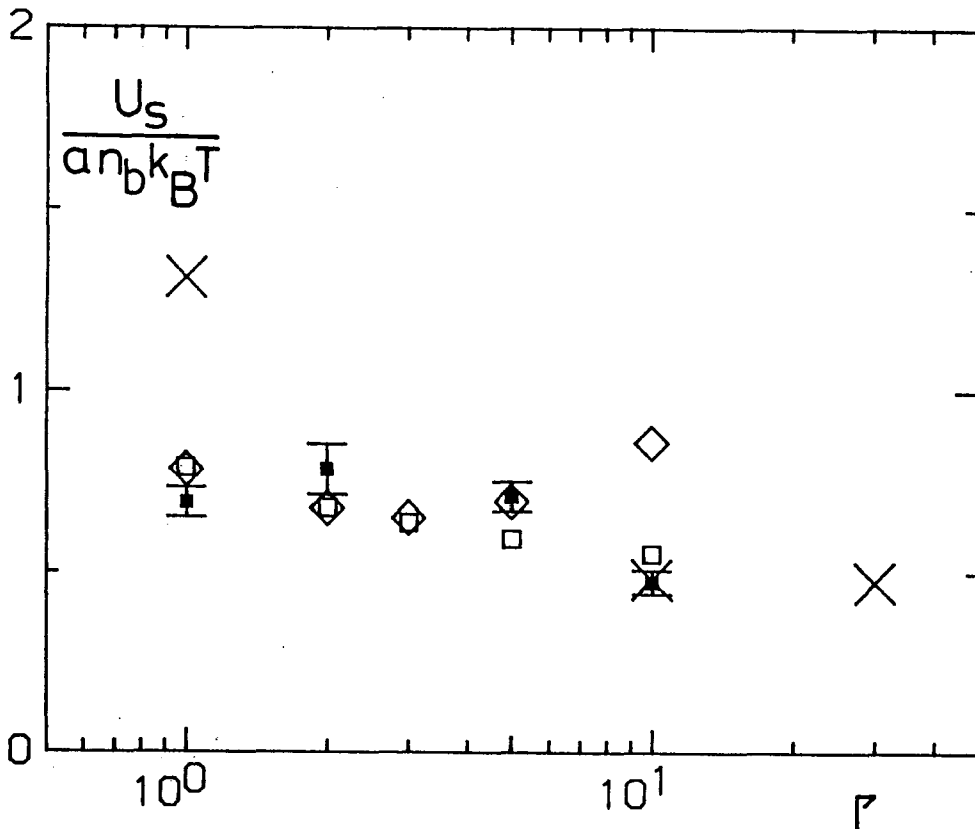


Fig.2. Surface energy density U_s normalized by $a n_b k_B T$: Present results (■) and those by Badiali et al.⁽¹⁾ (X) are compared with values obtained by the density-functional method (Rosinberg et al.⁽³⁾ (◇) and Hasegawa et al.⁽⁴⁾ (□)).

Table 4. Electrostatic potential

Γ	$eV(0)/k_B T$	$P/n_B k_B T$	$eV(\infty)/k_B T$
1	0.801	0.809	4.1
2	1.040	0.560	6.7
5	0.679	-0.252	5.2
10	-0.520	-1.666	-0.08

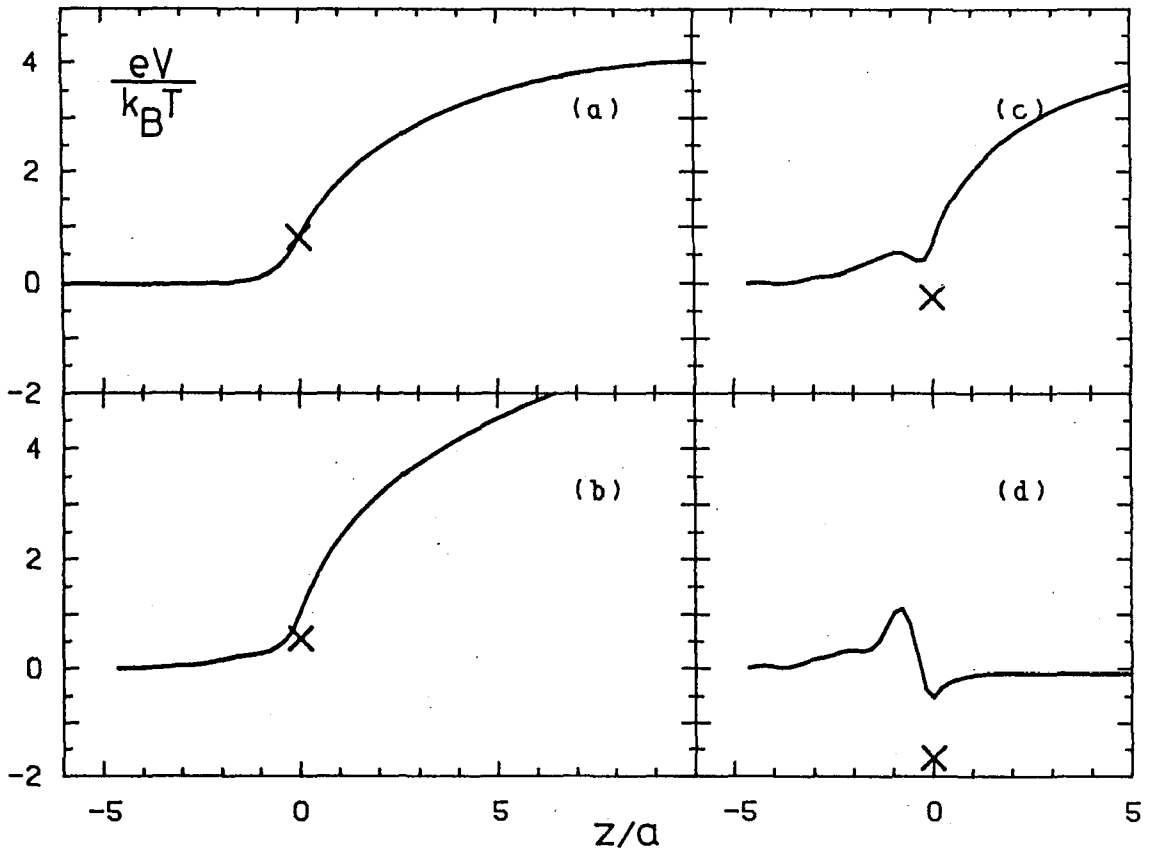


Fig.3. Electrostatic potential $V(z)$ normalized as $eV/k_B T$ for $\Gamma=1$ (a), 2 (b), 5 (c), and 10 (d) compared with the value required by exact relation (x).

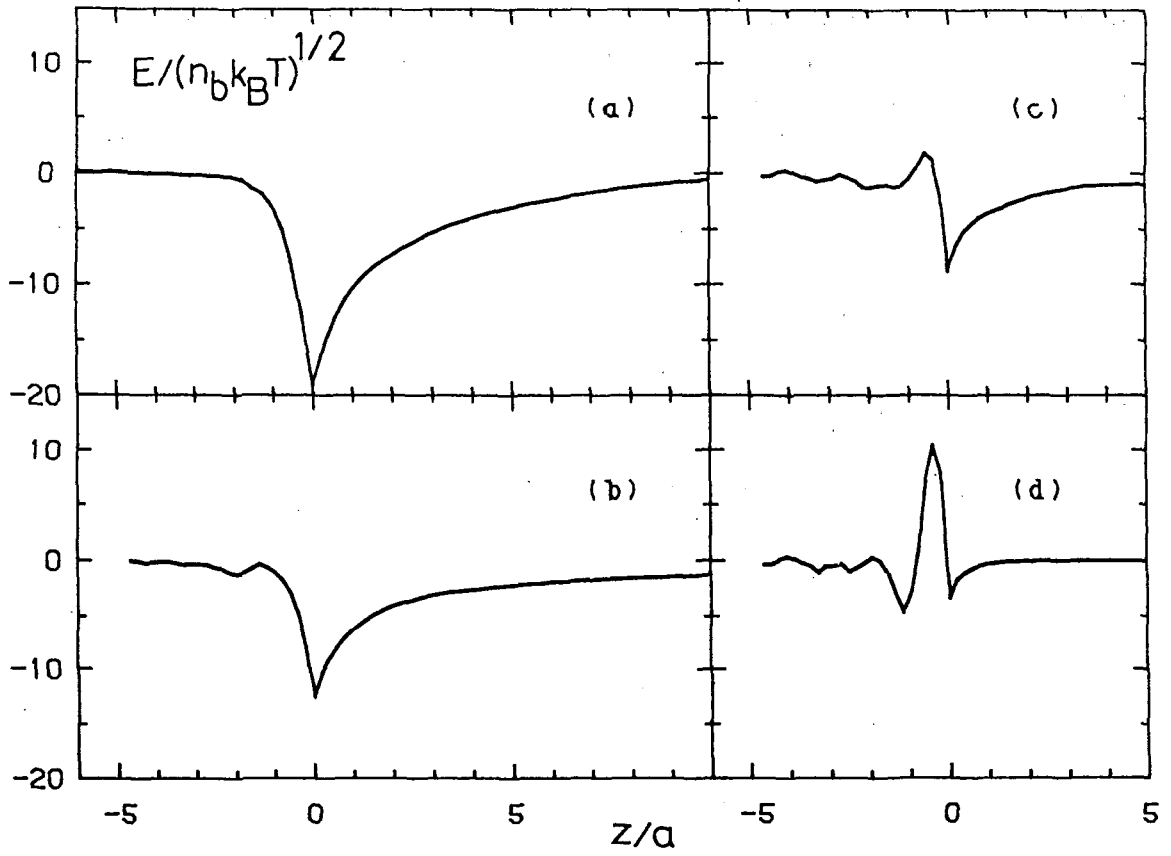


Fig.4. Electric field E normalized by $(n_b k_B T)^{1/2}$ for $\Gamma=1$ (a), 2(b), 5(c), and 10(d).

$$(1/2)e\Delta V/[e_c(\Gamma')+(1/2)eV(0)-e_c(\Gamma)]. \quad (17)$$

Here e_c is the bulk correlation energy per particle and $\Gamma' = (\rho(0)/n_b)^{1/3}\Gamma$. For $\Gamma=1, 2, 5,$ and 10 , the above expression is evaluated as $-0.01, +0.25, +0.28$ and $+0.18$.

We now compare our results for the surface energy with those of the density-functional calculations which are also shown in Fig.2. For $\Gamma=1$ and 10 , the surface energy is in agreement with but slightly smaller than calculated. When the effect of ΔV mentioned above is taken into account, values for $\Gamma=2$ and 5 are also roughly in agreement with calculations.

The consistency between the values of the potential obtained as a direct result of experiment and the exact relation has not been checked in earlier experiments. The above results indicate that this relation works as a useful guide to judge the reliability of experimental results.

4. CONCLUSION

We have made numerical experiments on the planar surface of the one-component plasma and checked the consistency of the results with the known exact relation between the potential and the bulk pressure. Conclusions may be as follows. (i) The surface energy of the planar surface for $\Gamma=1$ is about a half of that of spherical surface but the one for $\Gamma=10$ is almost the same. (ii) Our results are in rough agreement with the prediction of the density-functional theory but are slightly smaller for $\Gamma=1$ and 10 . (iii) The behavior of the potential near the surface should be consistent with the exact relation in order to obtain reliable values for the surface energy, and observation of the behavior of the density profile is not sufficient enough for the central part to have bulk properties. In order to obtain more reliable values for $\Gamma=2$ and 5 , experiments with increased system size may be necessary.

This work has been partially supported by the Grants-in-Aid for Scientific Researches of the Ministry of Education, Science, and Culture of Japan. Computations have been done at the Okayama University Computer Center and the Computer Center of the University of Tokyo. The author thanks Y. Yokoyama and T. Morishita for their

help in preparing figures.

REFERENCES

- (1) J. -P. Badiali, M.-L. Rosinberg, D. Levesque, and J. J. Weis J. Phys. C: Solid States Phys. 16(1983), 2183.
- (2) D. Levesque and J. J. Weis, J. Stat. Phys. 33(1983), 549.
- (3) M.-L. Rosinberg, J.-P. Badiali, and J. Goodisman, J. Phys. C: Solid State Phys. 16(1983), 4487.
- (4) M. Hasegawa and M. Watabe J. Phys. C: Solid State Phys. 18(1985), L573; *ibid.* 2081.
- (5) H. Totsuji, Phys. Rev. A 17(1978), 399.
- (6) N. Metropolis, A. W. Rosenbluth, M. N. Rosenbluth, A. H. Teller, and E. Teller, J. Chem. Phys. 21(1953), 1087.
- (7) P. Ballone, G. Senatore, and M. P. Tosi, Nuovo Cimento 65B(1981), 293.
- (8) H. Totsuji, J. Chem. Phys. 75(1981), 871.
- (9) W. L. Slattery, G. D. Doolen, and H. E. DeWitt, Phys. Rev. A 26(1982), 2255.